Author Manuscript

# Microbial metabolites, short-chain fatty acids, restrain tissue bacterial load, chronic inflammation, and associated cancer in the colon of mice

**Myunghoo Kim,[1] Leon Friesen,[1-2] Jeongho Park,[1] Hyungjin M. Kim,[3] and Chang H. Kim[1-2]**

[1]Department of Comparative Pathobiology and Purdue Research Center for Cancer Research, Purdue University, West Lafayette, IN 47907, U.S.A. [2]Laboratory of Immunology and Hematopoiesis, Department of Pathology and Mary H Weiser Food Allergy Center, University of Michigan School of Medicine, Ann Arbor, MI 48109, USA; [3]Department of Biostatistics, University of Michigan, Ann Arbor, MI 48109

Address Correspondence to Chang Kim, 109 Zina Pitcher Dr, Ann Arbor, MI 48109, USA; Phone: 734-615-8102; Email address: chhkim@umich.edu

Key words: Dietary fiber, Short-chain fatty acids, Inflammation, Colon cancer

Abbreviations: Abx, antibiotics; BM, bone marrow; AOM, azoxymethane; C2, acetate; C3, propionate; C4, butyrate; DF, dietary fiber; DSS, dextran sodium sulfate; HFD, high fiber diet; GPCR, G-protein-coupled receptors; LFD, low fiber diet; LP, lamina propria; MFD, medium fiber diet; SCFAs, short-chain fatty acids; q-PCR, quantitative PCR

**Abstract**

The intestinal immune system is regulated by microbes and their metabolites. The roles of gut microbial metabolites in regulating intestinal inflammation and tumorigenesis are

This is the author manuscript accepted for publication and has undergone full peer review but has not been through the copyediting, typesetting, pagination and proofreading process, which may lead to differences between this version and the Version of Record. Please cite this article as doi: 10.1002/eji.201747122.

This article is protected by copyright. All rights reserved.

Author Manuscript

incompletely understood. We systematically studied the roles of short-chain fatty acids (SCFAs) and their receptors (GPR43 or GPR41) in regulating tissue bacterial load, acute versus chronic inflammatory responses, and intestinal cancer development. SCFA receptor-, particularly GPR43-, deficient mice were defective in mounting appropriate acute immune responses to promote barrier immunity, and developed uncontrolled chronic inflammatory responses following epithelial damage. Further, intestinal carcinogenesis was increased in GPR43-deficient mice. Dietary fiber and SCFA administration suppressed intestinal inflammation and cancer in both GPR43-dependent and independent manners. The beneficial effect of GPR43 was not mediated by altered microbiota but by host tissue cells and hematopoietic cells to a lesser degree. We found that inability to suppress commensal bacterial invasion into the colonic tissue is associated with the increased chronic Th17-driven inflammation and carcinogenesis in the intestine of GPR43-deficient mice. In sum, our results reveal the beneficial function of the SCFA-GPR43 axis in suppressing bacterial invasion and associated chronic inflammation and carcinogenesis in the colon.

This article is protected by copyright. All rights reserved.

Author Manuscript

We found with animal models that dietary fiber, their microbial metabolites, and host receptors for these metabolites potentiate gut barrier immune responses during colon cancer development to decrease bacterial burden and chronic inflammatory responses, resulting in decreased cancer formation.

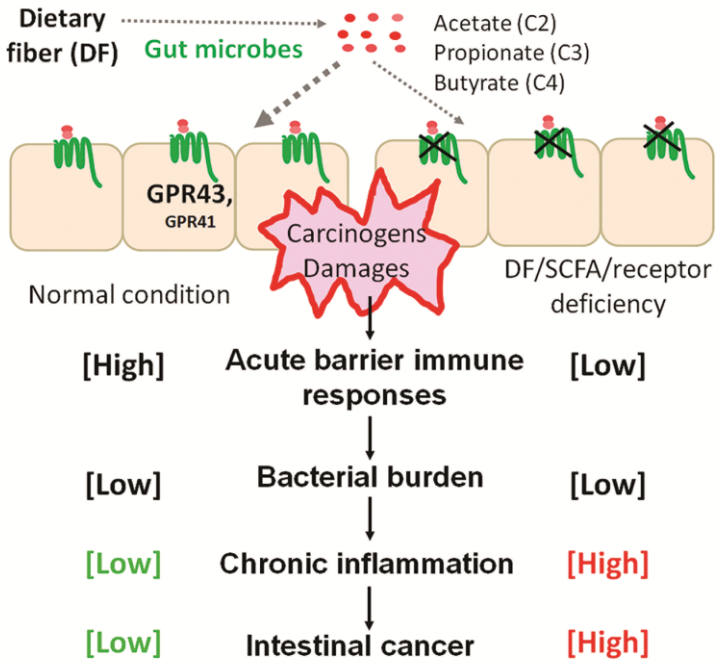


This article is protected by copyright. All rights reserved.

Author Manuscript

**Introduction**

The intestine harbors a myriad of commensal microorganisms, which benefit the host in many ways [1, 2]. Digestion resistant-dietary materials reach the colon for microbial fermentation. A major group of dietary materials processed by microbial fermentation includes dietary fibers (DF) and resistant starch. They are fermented to produce short-chain fatty acids (SCFAs), which play diverse roles from fueling colonocytes to regulating cells of the immune system, energy storage/metabolism, and gut barrier function [3-14].

SCFAs exert their functions in the host through both SCFA receptor-dependent and independent mechanisms [3]. SCFA receptors include G-protein-coupled receptors (GPCRs) such as GPR43, GPR41, GPR109A and Olfr78. GPR43 and GPR41 are activated by all major SCFAs such as acetate (C2), propionate (C3), and butyrate (C4) [15, 16]. GPR109A is activated by C4 along with a non-SCFA ligand, niacin [17]. Olfr78 is activated by C2 and C3, but not C4 [18]. Triggering these receptors induce activation of heterotrimeric G proteins and many downstream signaling molecules, including MAPK/ERK proteins [13, 16, 19, 20]. GPR43, GPR41 and GPR109A are differentially expressed by many cell types, including gut epithelial cells, macrophages, and dendritic cells [13, 15, 16]. Olfr78 is expressed in kidney endothelial cells [18].

Inflammation is a major risk factor for cancer development in the digestive tract [21-24]. Colon cancer is increased in patients with inflammatory bowel diseases, such as ulcerative colitis and Crohn's disease. Similarly, celiac disease and Crohn's disease are risk factors for small intestinal cancer. It has been documented that high SCFA levels and DF intake decrease colon cancer development [25]. GPR43 expression is decreased in tumor cells and this receptor functions to suppress colon cancer development [26-28]. Employing acute or chronic DSS-induced colitis models, two groups found that GPR43 has heterogeneous effects on dextran sodium sulfate (DSS)-induced inflammatory responses [29,

This article is protected by copyright. All rights reserved.

Author Manuscript

30]. GPR43 and GPR41 are required for mounting acute inflammatory responses following gut barrier breach [13, 29], which would be important for barrier repair and tissue bacterial clearance. GPR43 functions to increase beneficial *Bifidobacterium* species but suppress inflammatory *Helicobacter hepaticus* and *Prevotellaceae* [27], and cohousing of *Gpr43*$^{-/-}$ mice with wild type (WT) littermates suppressed acute 2% DSS-induced colitis [28]. However, it is also reported that DF suppress inflammation-associated colon cancer development in a manner independent of the microbiota change but dependent on another SCFA receptor GPR109A [31]. In this regard, DF or SCFA-receptor-associated microbiota effect on inflammation-associated colon cancer development is unknown. Moreover, the differential effect of the SCFA-SCFA receptor axis on acute versus chronic responses should be studied to better understand the working mechanisms of DF, SCFAs and their receptors in suppressing colon cancer development.

In this study, we addressed two critical issues regarding the role of the SCFA-SCFA receptor axis in regulating inflammation and cancer. First, we systematically determined the impact of SCFAs and their receptors, with the focus on GPR43, on tissue bacterial load and acute versus chronic inflammatory responses and how this relates to colon cancer development. Second, we interrogated whether the function of GPR43 is dependent on microbiota difference between WT and *Gpr43*$^{-/-}$ mice employing cohoused mice. Our work demonstrates the importance of the SCFA receptor-dependent barrier immunity in regulating bacterial invasion, subsequent inflammatory responses and colon cancer development in a microbiota change-independent manner.

This article is protected by copyright. All rights reserved.

Author Manuscript

## Results

### SCFA receptors promote acute but suppress chronic inflammatory responses

To systematically understand the roles of SCFA receptors in regulating inflammation, we compared the inflammatory responses of wild type (WT) and SCFA receptor (*Gpr43* and *Gpr41*)-deficient mice induced with DSS administered in acute and chronic inflammatory regimens. In response to an acute inflammation-inducing DSS treatment regimen (3.5% of DSS for 5 days and euthanized at day 9), SCFA receptor-deficient mice were hypo-responsive in mounting inflammatory responses at this early time point. Compared to WT mice, they lost less weight, had longer colons, failed to increase the frequencies of gut effector T cells (Th1 and Th17) and neutrophils, and did not up-regulate the mRNA expression of inflammatory cytokines and chemokines such as *Il18, Il22, Il6,* and *Cxcl1* (Figure 1; S. Fig. 1, 2A, B). Increased frequencies of Tregs were detected in *Gpr43*$^{-/-}$ mice. In general, *Gpr43*$^{-/-}$ mice were more defective in mounting the acute inflammatory response than *Gpr41*$^{-/-}$ mice.

In response to a chronic inflammation-inducing DSS treatment regimen (3 cycles of 1.5% DSS for 6 weeks), *Gpr43*$^{-/-}$ mice suffered less initially but more in the late phase based on weight change and stool score (Figure 2A). However, *Gpr41*$^{-/-}$ mice were not different from WT mice in the late phase. At termination following the chronic DSS treatment, *Gpr43*$^{-/-}$ mice had signs of more severe inflammation based on colon length and frequencies of inflammatory T cells (Th1 and Th17 cells) and neutrophils (Figure 2B-D, S. Fig 2C, D). In general, the expression of inflammatory cytokines, such as *Il18, Il22* and *Il6,* was higher in SCFA receptor-deficient mice (Figure 2E). Overall, these results indicate that the SCFA receptor GPR43 suppresses chronic inflammatory responses.

This article is protected by copyright. All rights reserved.

Author Manuscript

**GPR43 functions to suppress Th17-driven inflammatory response and intestinal carcinogenesis**

Inflammation induces production of cytokines and genotoxic reactive oxygen and nitrogen species, which cause mutations and epithelial damages. These events compromise gut barrier function and cause bacterial invasion, further increasing inflammatory responses leading to epithelial transformation [32-35]. Thus, we determined the impact of SCFA receptor deficiency on azoxymethane (AOM)/DSS-induced carcinogenesis. We found that *Gpr43*$^{-/-}$ mice initially suffered less from AOM/DSS-induced weight loss, and diarrhea the first 3-4 weeks but more in the late phase (Figure 3A, S Figure 3). The effect of GPR41 deficiency on cancer development was not as clear as in GPR43 deficiency, which mirrors the weak effect of GPR41 deficiency on chronic inflammation (S Figure 3 and Figure 2). Because of its clear function in suppressing DSS-induced chronic inflammation and AOM/DSS-induced cancer, we focused the remaining study on GPR43. At 10 weeks post-AOM treatment, *Gpr43*$^{-/-}$ mice had greater numbers of polyps and advanced (bigger) adenomas often with complete loss of crypts, medullary inflammatory cells (I) and necrotic abscesses (N) (Figure 3B and C). Further, they had enlarged spleen and mesenteric lymph nodes (MLN, Figure 3D), which indicate active systemic and intestinal inflammatory responses respectively.

It has been documented that GPR43-deficient mice have altered microbiota [27, 28] and, therefore, it is possible that the protective effect of GPR43 is mediated by the altered microbiota. To determine this, we induced AOM/DSS-induced colon cancer in co-housed mice and mice with shared bedding, both of which were effective in creating the same shared microbiota profile based on 16S rRNA gene q-PCR of selected bacterial groups such as Firmicutes (Lachnospiraceae), Firmicutes (Lactobacillus), Firmicutes (SFB), Bacteroidetes (Porphyromonadaceae), Bacteroidetes (*B. fragilis*), and Proteobacteria (Enterobacteriale) (S. Figure 4). *Gpr43*$^{-/-}$ mice maintained the same increased susceptibility to AOM/DSS-induced

This article is protected by copyright. All rights reserved.

Author Manuscript

colon cancer even after the microbiota-equalization procedures (Figure 4A, B). In the colon, the frequencies of Th17 cells and neutrophils were increased whereas there was no change in those of Th1 and FoxP3$^+$ Tregs (Figure 4C). In addition, increased organ weight and frequencies of Th1, Th17 and Treg cells were detected in the spleen and MLN, indicating elevated systemic and intestinal inflammation (Figure 4D,E). We also examined the immune cell profile at an early stage (16-17 days after AOM injection) in co-housed mice. We observed longer colon, somewhat decreased numbers of CD4$^+$ T cells and increased frequencies of Th17 cells in the colon of *Gpr43*$^{-/-}$ mice at this early stage of carcinogenesis (S Figure 5). Thus, sustained high Th17-driven inflammatory response is the characteristic phenotype of *Gpr43*$^{-/-}$ mice during the colon cancer development. Importantly, this phenotype was detected in the absence of microbial changes due to GPR43 deficiency.

Next, we employed another intestinal cancer model (*APC*$^{Min/+}$ mice) to verify the protective role of GPR43. This model develops spontaneous adenomas in both the small intestine and colon. *Gpr43*$^{-/-}$ *APC*$^{Min/+}$ mice developed more tumors in the small intestine and colon than *APC*$^{Min/+}$ mice, with greater numbers of adenomas (Figure 5A, C). Histological analysis revealed disordered epithelial cancer continuous from intestinal crypts in the intestine of *Gpr43*$^{-/-}$ *APC*$^{Min/+}$ mice (Figure 5B). The spleen and MLN of *Gpr43*$^{-/-}$ *APC*$^{Min/+}$ mice were abnormally enlarged (Figure 5D).

*Gpr43* is expressed by both tissue cells and hematopoietic cells, including gut epithelial cells, enteroendocrine L cells, adipocytes, eosinophils, basophils, neutrophils, monocytes, dendritic cells, mucosal mast cells, and myometrium endothelium [3]. To determine the relative importance of tissue versus hematopoietic cells in mediating the protective function of GPR43 on colon cancer, we performed a bone marrow (BM) transplantation study. We induced colon cancer with AOM/DSS in these mice and measured weight change, survival, tumor burden, and lymphoid tissue enlargement. While differences

This article is protected by copyright. All rights reserved.

Author Manuscript

between groups in not all the readouts were statistically significant, there was a trend that the "*Gpr43*$^{-/-}$ (BM donor)→*Gpr43*$^{-/-}$ (recipient)" group was most susceptible, followed by the "WT→*Gpr43*$^{-/-}$" group, and then by the "*Gpr43*$^{-/-}$ →WT" group (Figure 6). Thus, both cell types may mediate the protective effect of GPR43, but it was the non-hematopoietic tissue cells that play a major role.

**GPR43 partially mediates the protective effect of DF and SCFAs**

DF and SCFAs have SCFA receptor-independent functions. For example, SCFAs function as HDAC inhibitors or metabolic regulators [36], which do not require SCFA receptors. To determine if the protective effect of DF on AOM/DSS-induced colon cancer is GPR43-dependent, WT and *Gpr43*$^{-/-}$ mice were fed low-fiber diet (LFD, 0% soluble DF: 1:1= pectin and inulin), medium-fiber diet (MFD, 5% soluble DF), or high-fiber diet (HFD,15% soluble DF) and were examined for their susceptibility to AOM/DSS-induced carcinogenesis. As demonstrated in the literature, DF suppresses colon cancer development in WT mice in a dose-dependent manner (Figure 7). DF also suppressed carcinogenesis in *Gpr43*$^{-/-}$ mice but this effect was smaller than that in WT. This indicates that DF can suppress carcinogenesis in both *Gpr43*-dependent and independent manners.

We next studied if GPR43 mediates the protective effect of C3. C3 was chosen because it is a high affinity ligand for GPR43 and an efficient inhibitor of HDACs [15, 16, 37]. The increased AOM/DSS-induced cancer development, along with spleen enlargement, in LFD-fed WT mice was suppressed by C3 administered in drinking water (Figure 8A and B). C3 decreased cancer formation and spleen enlargement in WT mice and in *Gpr43*$^{-/-}$ mice to a lesser degree (Figure 8C and E). Interestingly, C3 and DF (i.e. MFD) had additive suppressive effects on cancer development and spleen enlargement (Figure 8C-E). Overall

This article is protected by copyright. All rights reserved.

Author Manuscript

these results indicate that DF and C3 suppress cancer development in *Gpr43*-dependent and independent manners.

**Increased tissue bacterial load contributes to intestinal carcinogenesis in *Gpr43*$^{-/-}$ mice**

Defective regulation of gut permeability in inflammatory conditions has been reported for *Gpr43*$^{-/-}$ mice [13]. We found that the expression of *ocln* (the gene for Occludin) at mRNA level was greatly decreased in the colon of *Gpr43*$^{-/-}$ mice after 3 cycles of 1.5% DSS treatment (Figure 9A). C3 increased the expression of *ocln* and *tjp1* (the gene for ZO-1) in the colon of WT mice but failed to increase their expression in *Gpr43*$^{-/-}$ mice. Consistently, gut permeability was higher in *Gpr43*$^{-/-}$ than WT mice following the chronic DSS treatment (Figure 9B). We performed fluorescent in situ hybridization (FISH) for eubacterial 16S RNA gene and quantitative (q)-PCR analysis to detect bacteria in colon tissues. The abnormal gut permeability in *Gpr43*$^{-/-}$ mice was supported by increased levels of eubacteria in colon tissues (Figure 9C). We found that many more bacteria were detected within the colon tissues of *Gpr43*$^{-/-}$ compared to WT mice during chronic inflammation. Importantly, C3 feeding decreased tissue bacteria (Figure 9C). We also examined tissue bacteria during AOM/DSS-induced carcinogenesis in the colon. Tissue bacterial load was not different in co-housed WT and *Gpr43*$^{-/-}$ mice at an early stage but later it was decreased in WT but remained elevated in *Gpr43*$^{-/-}$ mice (Figure 9D), indicating defective control of tissue bacterial load at the chronic stage in GPR43 deficiency.

To understand the role of the increased tissue bacteria in *Gpr43*$^{-/-}$ mice, mice were treated with antibiotics during intestinal carcinogenesis. Antibiotics suppressed AOM/DSS-induced colon cancer in *Gpr43*$^{-/-}$ mice (Figure 9E). Antibiotics suppressed the numbers of tumors in *Gpr43*$^{-/-}$ mice than that not in WT mice. Antibiotics also significantly decreased the

This article is protected by copyright. All rights reserved.

Author Manuscript

enlargement of spleen in *Gpr43*$^{-/-}$ mice (not shown). Overall, these results indicate that increased colon cancer formation in *Gpr43*$^{-/-}$ mice is due in part to high levels of tissue bacteria.

**Discussion**

We studied, in depth, the impact of DF, SCFAs, and SCFA receptors on tissue bacterial load, intestinal inflammation and carcinogenesis. Based on early *in vitro* data with cell lines, it has been proposed that SCFAs inhibit HDACs to suppress cancer cells [38-40]. However, this mechanism alone does not fully explain the SCFA effect on carcinogenesis *in vivo*. A mounting body of evidence, including the data presented in this report, suggests that the protective effect of SCFAs is, in part, mediated by SCFA receptors [27, 31], which function in a largely HDAC-independent manner. We found that SCFAs and SCFA receptors promote barrier immunity and suppress bacterial invasion, which can induce chronic inflammatory responses. Importantly, SCFAs, exemplified by C3, and GPR43 have suppressive effects on chronic inflammatory responses and intestinal carcinogenesis.

We studied both GPR43 and GPR41 but focused our efforts on GPR43 because the anti-cancer effect of GPR43 was greater than that of GPR41. The two GPCRs are receptors for C2, C3 and C4 but their affinity to these SCFAs are different [16]. While both receptors are expressed by intestinal epithelial cells, the distribution of the two in the body are very different [3, 37]. For example, GPR43 is expressed by neutrophils, whereas GPR41 is expressed by adipocytes. Also, the two may be expressed by different cell types in the intestine. These differences in receptor expression are likely to account for the observed differences in SCFA receptor functions. Our BM transplantation experiment revealed that non-BM-derived tissue cells play a major role in mediating the GPR43-dependent suppression of intestinal inflammation and carcinogenesis, while hematopoietic cells play a

This article is protected by copyright. All rights reserved.

Author Manuscript

relatively minor role. The most likely cells to mediate the GPR43 function are intestinal epithelial cells, which highly express GPR43 and are effectively stimulated by SCFAs for barrier immunity [13]. This finding is in line with a previous report that non-hematopoietic cells are the major mediator of the GPR109A effect [31]. However, a minor but significant role of hematopoietic cells was still observed in both studies.

SCFAs promote the expression of intestinal tight junction proteins in the steady state and boost anti-microbial responses during infection or following gut barrier breach [14, 41]. T cell responses in the intestine reflect the inflammatory status regulated by SCFAs and their receptors. Particularly, Th17 cells, which contribute to barrier immunity, undergo expansion during an acute phase of immune responses but contraction as inflammatory responses subside. Numbers of Th17 cells remain increased in *Gpr43*$^{-/-}$ mice along with chronic inflammation. This effect somewhat mirrors that of GPR109A [31]. These results identify important roles of SCFAs and their receptors in mounting innate and adaptive immune responses to suppress bacterial invasion across the barrier. The increased Th17 cell response in GPR43 deficiency appears to be a bystander response as the consequence of inflammatory responses due to bacterial invasion but we cannot rule out the possibility that it may involve antigen-specific responses. This finding clarifies the rather unexpected attenuated inflammation observed by Sina et al at an acute phase of DSS-induced inflammation [29]. It has been recently reported that GPR43 and GPR109A promote epithelial inflammasome responses [28]. Our results together with these reports emphasize the defective acute inflammatory response and associated-gut permeability change in *Gpr43*$^{-/-}$ mice following DSS or AOM/DSS treatment, observed in this study

Sustained high bacterial burden in colon tissues can cause chronic inflammatory responses. For example, inflammatory cytokines and chemokines, such as IL-18, IL-22, IL-6 and CXCL1, which promote effective barrier immunity to ward off invading bacteria [42-44],

This article is protected by copyright. All rights reserved.

Author Manuscript

were not normally induced at the early phase in *Gpr43*$^{-/-}$ mice. During prolonged treatments with DSS or AOM/DSS, *Gpr43*$^{-/-}$ mice suffer less than WT mice in the first few weeks but become more susceptible afterward. This indicates that SCFA receptors function to coordinately regulate acute and chronic inflammatory responses. The function of SCFA receptors in regulating chronic inflammation is closely related to their function in suppressing intestinal cancer. In *APC*$^{min/+}$ mice, tumors are formed more in the small, than large, intestine, and thus this model provides additional insights into SCFA-receptor-regulated cancer outside the colon. The phenotype of this model indicates that the SCFA-GPR43 axis has anti-cancer effects in both the small and large intestines.

Inflammation is frequently linked to carcinogenesis. Our results indicate that DF and SCFAs, as represented by C3 in this study, suppress intestinal cancer in GPR43-dependent and independent manners. Our findings are in line with others' findings that DF, SCFAs and SCFA receptors exert suppressive effects on colon cancer [27, 31, 45-48] and provide a potential mechanism for the suppressive function. Our findings underscore the important role of the SCFA- SCFA receptor axis in suppressing bacterial invasion, subsequent chronic inflammation and inflammation-associated intestinal carcinogenesis. Colon cancer development is closely associated with gut microbiota changes [49-51]. DF changes the gut microbiota. For example, DF enriches *Bacteroidaceae* and *Bifidobacteriaceae* and potentially decrease pathogenic bacteria [52]. *Firmicutes*, particularly those of the *Erysipelotrichaceae* family, are increased in DF deficiency. Moreover, GPR43 functions to increase beneficial bacterial species [27]. In this study, co-housing with WT-littermates failed to suppress the elevated chronic Th17 response, bacterial invasion and associated colon cancer development in *Gpr43*$^{-/-}$ mice in response to AOM/DSS-treatment. This indicates that control of the microbiota by GPR43 does not have a dominant role on colon cancer development. Rather, the data underline the importance of host cells in mediating the

This article is protected by copyright. All rights reserved.

Author Manuscript

protective effect of GPR43. We conclude that the SCFA-GPR43 axis functions to boost barrier immune responses against microbiota and this response limits persistent bacterial invasion, chronic inflammatory responses and colon cancer development.

## Materials and Methods

### Mice, diet and SCFA administration

All animal experiments were approved by the Purdue Animal Care and Use Committee (PACUC). CD45.1 C57BL/6 mice and *Apc*$^{Min/+}$ mice were from the Jackson Laboratory (Bar Harbor, ME). *Gpr43*$^{-/-}$ mice were purchased from Deltagen (San Mateo, CA), and *Gpr41*$^{-/-}$ mice were obtained from Dr. M Yanagisawa (UT Southwestern Medical Center at Dallas). All mice were on C57BL/6 background. *Gpr43*$^{-/-}$ mice were crossed with *Apc*$^{Min/+}$ mice to derive *Apc*$^{Min/+}$*Gpr43*$^{-/-}$ mice. The mice were kept at the Purdue Life Science Animal Facility for at least 12 months prior to the study. Mice were fed regular rodent chow (Harlan 2018S Global 18% Protein Rodent Diet) or special DF diets. The special diets containing different amounts of DF (0% of pectin and inulin at 1:1 ratio for LFD, 5% for MFD, and 15% for HFD) were custom-ordered from Envigo. Mice were fed special diets from 3 weeks of age and/or drinking water containing C3 (80 mM, pH 7.4). Mice were treated with DSS or AOM/DSS from 5 or 6 weeks of age for most mice or 11-12 weeks of age for BM chimera mice. When indicated, mice were treated with antibiotics (ampicillin, neomycin, and metronidazole at 1 g/L and vancomycin at 0.5 g/L). When indicated (Figure 4, 9D, and Supporting Figure 2), female mice were co-housed for 1-2 weeks before and during the induction of AOM/DSS-induced colon cancer. Alternatively, WT and *Gpr43*$^{-/-}$ mice were housed in cages inoculated with mixed soiled bedding from WT and *Gpr43*$^{-/-}$ mice (20% old

This article is protected by copyright. All rights reserved.

mixed and 80% new bedding; changed every 3-4 days). The data obtained with the two methods were similar and therefore were combined.

**DSS-induced acute and chronic intestinal inflammation**

For acute intestinal inflammation, mice were on 3.5% DSS in drinking water for 5 days and then on plain water before they were euthanized on day 9. For chronic intestinal inflammation, mice were treated with 1.5% DSS in drinking water for 7 days and then with regular water for 7 days. This cycle was repeated three times. Intestinal tissues were examined by flow cytometry for T cells and neutrophils and by qRT-PCR for expression of inflammatory cytokines (IL-6, IL-18, IL-22, and CXCL-1) as described previously [13, 53]. Primers used for this study were previously described [13].

**Tight junction proteins, tissue bacterial burden, and cecal bacterial 16S rRNA gene PCR analysis**

Mice were assessed for expression of tight junction protein genes (*ocln* and *tjp1*), gut permeability, and tissue bacteria 42 days after the start of DSS treatment. The expression of *ocln* and *tjp1*was determined by qRT-PCR with the primers: ACC ACT ATG AAA CAG ACT ACA CG (Ocln-F), GGA GAA CTA CAC GCT ATT AAA CG (Ocln-R), GAA GAT GAA GAT GAG GAT GGT CA (tjp1-F), ACC AGT GAT TAG TCC TGT CTT TGT (tjp1-R). Tissue bacterial levels were determined by q-PCR of a common eubacterial 16S rRNA gene sequences and normalized by genomic β-actin levels as previously described [13]. Cecal bacterial 16S rRNA gene PCR analysis for cohoused animals was performed as described previously [13, 54].

Author Manuscript

This article is protected by copyright. All rights reserved.

Author Manuscript

**Gut permeability**

For assessing gut permeability, mice were fasted overnight and orally gavaged with fluorescein isothiocyanate (FITC)–conjugated dextran (0.2 mg/g of body weight, mean molecular weight of 3000–5000; Sigma- Aldrich, St Louis, MO) using a round-tip feeding needle. Mice were sacrificed 3 h later, and the FITC-dextran concentration in the plasma was determined with a fluorescent microplate reader (excitation at 485 nm and emission at 535 nm; Synergy HT; BioTek, Winooski, VT).

**AOM/DSS and *APC*$^{Min/+}$-induced models of intestinal cancer**

Mice were treated i.p. with azoxymethane (AOM, 10 mg/kg of body weight) and rested for 7 days. The mice were then administered with 1% DSS (36–50 kDa) in drinking water for 7 days and rested on regular water for 7 days. This cycle was repeated 3 times. Mice were monitored daily for changes in body weight, signs of illness, and stool score. Mice were sacrificed 62-70 days post-AOM injection and were assessed for polyp size and number and organ (spleen and MLN) weight. Colon tissues were paraffin-embedded and tissue sections were stained with hematoxylin and eosin. *Apc*$^{Min/+}$ mice and *Apc*$^{Min/+}$*Gpr43*$^{-/-}$ mice were similarly assessed for tumors in the small and large bowels and organ weight at 4 months of age.

**Cell isolation and flow cytometry**

For isolation of intestinal LP cells, intestinal tissues were harvested into cold PBS and trimmed to remove mesenteries, fat, and Peyer's patches. Intestinal tissues were cut into ~2 cm pieces. The epithelial layer was extracted five times with 10 mM EDTA in HBSS buffer at room temperature for 15 min, and then the remaining tissues were digested twice at 37°C

This article is protected by copyright. All rights reserved.

Author Manuscript

for 1 hour with 1.5 mg/ml collagenase (type 3, Worthington). Collected cells were stained with antibodies to Gr-1 (RB6-8C5), CD11b (M1/70) and CD45 (30-F11) for neutrophils or to CD4 (RM4-5) for T cells. For intracellular staining of IL-17 and IFN-γ, cells were activated in RPMI 1640 (10% fetal bovine serum) with phorbol myristate acetate (50 ng/ml), ionomycin (1 mM), and monensin (2mM; Sigma- Aldrich) for 4 h. Cells were then fixed, permeabilized, and stained with antibodies to mIL-17A (TC11-18H10.1) or IFNγ (XMG1.2). For FoxP3 staining, cells were fixed, permeabilized, and then stained with FoxP3 (FJK-16S) according to the manufacturer's protocol (eBioscience). Detailed gating strategies are found in S. Fig. 1.

**Bone marrow transplantation**

To prepare host mice, WT or *Gpr43*$^{-/-}$ mice were irradiated at 500 rads, and this was repeated after 4 h. Host mice were injected i.v. with $1 \times 10^7$ BM cells from WT or *Gpr43*$^{-/-}$ mice. The CD45.1 and CD45.2 congenic system was used to distinguish donor and recipient cells. Six weeks later, mice were checked for hematopoietic reconstitution and were treated with AOM and DSS. The marrow reconstitution efficiency in these animals was >95% (spleen).

**Confocal microscopy and histological analysis**

Colon tissues, harvested from WT or *Gpr43*$^{-/-}$ mice subjected to chronic DSS treatment, were frozen in Tissue-Tek OCT compound (Sakura) and were cut into 8-μm sections. The sections were fixed in cold acetone and stained with CY3-labled EU338 (5′ -GCT GCC TCC CGT AGG AGT-3, Eurofins) and Pan-cytokeratin. Confocal images were collected with a SP5 II laser scanning microscopic system (Leica). For histological analysis, sections (6 μm) of

This article is protected by copyright. All rights reserved.

Author Manuscript

paraffin-embedded intestinal tissues were stained with hematoxylin and eosin. Histological images were taken at 50× magnification.

**Statistical analysis**

For weight change and stool score, repeated measures ANOVA was used to determine group effects (Figure 1A, 2A, 3A, 6A, and 7B) for indicated time periods, and after finding a significant group effect, pairwise comparisons of interest on specific days were made using two-sample t-tests with Bonferroni's adjustments to account for multiple comparisons. For analyzing Figure 8C, 8E, and 9, two-way ANOVA was used with an interaction of the two factors, and upon a significant interaction, multiple pairwise comparisons were made using t-tests with Bonferroni adjustments. When no interaction is evident, results from two-way ANOVA with main effects only are presented. For comparing multiple groups in Figure 1B-E, 2B-E, 6B, 6C and 7C, one-way ANOVA followed by Tukey's multiple comparisons test was used. Additionally, Mann-Whitney U-test (two-sided with statistical significance set at 0.05) was used to compare two groups of interest (Figure 3B, 3D, 4, 5C, 5D, 8A, and 8B). All error bars indicate SEM. Prism (Graphpad) and SAS (SAS) statistical software were used.

**Acknowledgments:** We thank ST Park for his helpful assistance with animal experiments and tissue preparation. This study was supported, in part, from grants from Purdue Center for Cancer Research (Challenge Award) and NIH (1R01AI121302, R01AI080769, and 1S10RR02829) to CHK.

**Conflict of interest:** The authors declare no financial or commercial conflicts of interest.

This article is protected by copyright. All rights reserved.

Author Manuscript

**References**


1 **Zeng, M. Y., Inohara, N. and Nunez, G.,** Mechanisms of inflammation-driven bacterial dysbiosis in the gut. *Mucosal Immunol* 2016.

2 **Wroblewski, L. E., Peek, R. M., Jr. and Coburn, L. A.,** The Role of the Microbiome in Gastrointestinal Cancer. *Gastroenterol Clin North Am* 2016. **45**: 543-556.

3 **Kim, C. H., Park, J. and Kim, M.,** Gut microbiota-derived short-chain Fatty acids, T cells, and inflammation. *Immune network* 2014. **14**: 277-288.

4 **Louis, P., Hold, G. L. and Flint, H. J.,** The gut microbiota, bacterial metabolites and colorectal cancer. *Nat Rev Microbiol* 2014. **12**: 661-672.

5 **Topping, D. L. and Clifton, P. M.,** Short-chain fatty acids and human colonic function: roles of resistant starch and nonstarch polysaccharides. *Physiol Rev* 2001. **81**: 1031-1064.

6 **Sun, M., Wu, W., Liu, Z. and Cong, Y.,** Microbiota metabolite short chain fatty acids, GPCR, and inflammatory bowel diseases. *J Gastroenterol* 2016.

7 **Koh, A., De Vadder, F., Kovatcheva-Datchary, P. and Backhed, F.,** From Dietary Fiber to Host Physiology: Short-Chain Fatty Acids as Key Bacterial Metabolites. *Cell* 2016. **165**: 1332-1345.

8 **Morrison, D. J. and Preston, T.,** Formation of short chain fatty acids by the gut microbiota and their impact on human metabolism. *Gut Microbes* 2016. **7**: 189-200.

9 **Ruppin, H., Bar-Meir, S., Soergel, K., Wood, C. and Schmitt Jr, M.,** Absorption of short-chain fatty acids by the colon. *Gastroenterology* 1980. **78**: 1500-1507.

10 **Frost, G., Sleeth, M. L., Sahuri-Arisoylu, M., Lizarbe, B., Cerdan, S., Brody, L., Anastasovska, J., Ghourab, S.,** The short-chain fatty acid acetate reduces appetite via a central homeostatic mechanism. *Nat Commun* 2014. **5**: 3611.

11 **Perry, R. J., Peng, L., Barry, N. A., Cline, G. W., Zhang, D., Cardone, R. L., Petersen, K. F., Kibbey, R. G.,** Acetate mediates a microbiome-brain-beta-cell axis to promote metabolic syndrome. *Nature* 2016. **534**: 213-217.

12 **De Vadder, F., Kovatcheva-Datchary, P., Goncalves, D., Vinera, J., Zitoun, C., Duchampt, A., Backhed, F. and Mithieux, G.,** Microbiota-generated metabolites promote metabolic benefits via gut-brain neural circuits. *Cell* 2014. **156**: 84-96.

13 **Kim, M. H., Kang, S. G., Park, J. H., Yanagisawa, M. and Kim, C. H.,** Short-chain fatty acids activate GPR41 and GPR43 on intestinal epithelial cells to promote inflammatory responses in mice. *Gastroenterology* 2013. **145**: 396-406 e391-310.

14 **Kelly, C. J., Zheng, L., Campbell, E. L., Saeedi, B., Scholz, C. C., Bayless, A. J., Wilson, K. E., Glover, L. E.,** Crosstalk between Microbiota-Derived Short-Chain Fatty Acids and Intestinal Epithelial HIF Augments Tissue Barrier Function. *Cell Host Microbe* 2015. **17**: 662-671.

15 **Brown, A. J., Goldsworthy, S. M., Barnes, A. A., Eilert, M. M., Tcheang, L., Daniels, D., Muir, A. I., Wigglesworth, M. J.,** The Orphan G protein-coupled receptors GPR41 and GPR43 are activated by propionate and other short chain carboxylic acids. *J Biol Chem* 2003. **278**: 11312-11319.

16 **Le Poul, E., Loison, C., Struyf, S., Springael, J. Y., Lannoy, V., Decobecq, M. E., Brezillon, S., Dupriez, V.,** Functional characterization of human receptors for short chain fatty acids and their role in polymorphonuclear cell activation. *J Biol Chem* 2003. **278**: 25481-25489.


This article is protected by copyright. All rights reserved.

Author Manuscript

17 **Wise, A., Foord, S. M., Fraser, N. J., Barnes, A. A., Elshourbagy, N., Eilert, M., Ignar, D. M., Murdock, P. R.,** Molecular identification of high and low affinity receptors for nicotinic acid. *J Biol Chem* 2003. **278**: 9869-9874.

18 **Pluznick, J. L., Protzko, R. J., Gevorgyan, H., Peterlin, Z., Sipos, A., Han, J., Brunet, I., Wan, L. X.,** Olfactory receptor responding to gut microbiota-derived signals plays a role in renin secretion and blood pressure regulation. *Proc Natl Acad Sci U S A* 2013. **110**: 4410-4415.

19 **Yonezawa, T., Kobayashi, Y. and Obara, Y.,** Short-chain fatty acids induce acute phosphorylation of the p38 mitogen-activated protein kinase/heat shock protein 27 pathway via GPR43 in the MCF-7 human breast cancer cell line. *Cell Signal* 2007. **19**: 185-193.

20 **Seljeset, S. and Siehler, S.,** Receptor-specific regulation of ERK1/2 activation by members of the "free fatty acid receptor" family. *J Recept Signal Transduct Res* 2012. **32**: 196-201.

21 **Hartnett, L. and Egan, L. J.,** Inflammation, DNA methylation and colitis-associated cancer. *Carcinogenesis* 2012. **33**: 723-731.

22 **Werts, C., Rubino, S., Ling, A., Girardin, S. E. and Philpott, D. J.,** Nod-like receptors in intestinal homeostasis, inflammation, and cancer. *J Leukoc Biol* 2011. **90**: 471-482.

23 **Ullman, T. A. and Itzkowitz, S. H.,** Intestinal inflammation and cancer. *Gastroenterology* 2011. **140**: 1807-1816.

24 **Landgren, A. M., Landgren, O., Gridley, G., Dores, G. M., Linet, M. S. and Morton, L. M.,** Autoimmune disease and subsequent risk of developing alimentary tract cancers among 4.5 million US male veterans. *Cancer* 2011. **117**: 1163-1171.

25 **Park, Y., Hunter, D. J., Spiegelman, D., Bergkvist, L., Berrino, F., van den Brandt, P. A., Buring, J. E., Colditz, G. A.,** Dietary fiber intake and risk of colorectal cancer: a pooled analysis of prospective cohort studies. *JAMA* 2005. **294**: 2849-2857.

26 **Tang, Y., Chen, Y., Jiang, H., Robbins, G. T. and Nie, D.,** G-protein-coupled receptor for short-chain fatty acids suppresses colon cancer. *Int J Cancer* 2011. **128**: 847-856.

27 **Sivaprakasam, S., Gurav, A., Paschall, A. V., Coe, G. L., Chaudhary, K., Cai, Y., Kolhe, R., Martin, P.,** An essential role of Ffar2 (Gpr43) in dietary fibre-mediated promotion of healthy composition of gut microbiota and suppression of intestinal carcinogenesis. *Oncogenesis* 2016. **5**: e238.

28 **Macia, L., Tan, J., Vieira, A. T., Leach, K., Stanley, D., Luong, S., Maruya, M., Ian McKenzie, C.,** Metabolite-sensing receptors GPR43 and GPR109A facilitate dietary fibre-induced gut homeostasis through regulation of the inflammasome. *Nat Commun* 2015. **6**: 6734.

29 **Sina, C., Gavrilova, O., Forster, M., Till, A., Derer, S., Hildebrand, F., Raabe, B., Chalaris, A.,** G protein-coupled receptor 43 is essential for neutrophil recruitment during intestinal inflammation. *J Immunol* 2009. **183**: 7514-7522.

30 **Maslowski, K. M., Vieira, A. T., Ng, A., Kranich, J., Sierro, F., Yu, D., Schilter, H. C., Rolph, M. S.,** Regulation of inflammatory responses by gut microbiota and chemoattractant receptor GPR43. *Nature* 2009. **461**: 1282-1286.

31 **Singh, N., Gurav, A., Sivaprakasam, S., Brady, E., Padia, R., Shi, H., Thangaraju, M., Prasad, P. D.,** Activation of Gpr109a, receptor for niacin and the commensal metabolite butyrate, suppresses colonic inflammation and carcinogenesis. *Immunity* 2014. **40**: 128-139.

This article is protected by copyright. All rights reserved.

Author Manuscript


32 **Janakiram, N. B. and Rao, C. V.,** The role of inflammation in colon cancer. *Adv Exp Med Biol* 2014. **816**: 25-52.

33 **Ohnishi, S., Ma, N., Thanan, R., Pinlaor, S., Hammam, O., Murata, M. and Kawanishi, S.,** DNA damage in inflammation-related carcinogenesis and cancer stem cells. *Oxid Med Cell Longev* 2013. **2013**: 387014.

34 **Brennan, C. A. and Garrett, W. S.,** Gut Microbiota, Inflammation, and Colorectal Cancer. *Annu Rev Microbiol* 2016. **70**: 395-411.

35 **Greten, F. R., Eckmann, L., Greten, T. F., Park, J. M., Li, Z. W., Egan, L. J., Kagnoff, M. F. and Karin, M.,** IKKbeta links inflammation and tumorigenesis in a mouse model of colitis-associated cancer. *Cell* 2004. **118**: 285-296.

36 **Licciardi, P. V., Ververis, K. and Karagiannis, T. C.,** Histone deacetylase inhibition and dietary short-chain Fatty acids. *ISRN Allergy* 2011. **2011**: 869647.

37 **Park, J., Kim, M., Kang, S., Jannasch, A., Cooper, B., Patterson, J. and Kim, C.,** Short-chain fatty acids induce both effector and regulatory T cells by suppression of histone deacetylases and regulation of the mTOR–S6K pathway. *Mucosal immunology* 2015. **8**: 80-93.

38 **Hinnebusch, B. F., Meng, S., Wu, J. T., Archer, S. Y. and Hodin, R. A.,** The effects of short-chain fatty acids on human colon cancer cell phenotype are associated with histone hyperacetylation. *J Nutr* 2002. **132**: 1012-1017.

39 **Shao, Y., Gao, Z., Marks, P. A. and Jiang, X.,** Apoptotic and autophagic cell death induced by histone deacetylase inhibitors. *Proc Natl Acad Sci U S A* 2004. **101**: 18030-18035.

40 **Fung, K. Y., Brierley, G. V., Henderson, S., Hoffmann, P., McColl, S. R., Lockett, T., Head, R. and Cosgrove, L.,** Butyrate-induced apoptosis in HCT116 colorectal cancer cells includes induction of a cell stress response. *J Proteome Res* 2011. **10**: 1860-1869.

41 **Sun, Y. and O'Riordan, M. X.,** Regulation of bacterial pathogenesis by intestinal short-chain Fatty acids. *Adv Appl Microbiol* 2013. **85**: 93-118.

42 **Rubino, S. J., Geddes, K. and Girardin, S. E.,** Innate IL-17 and IL-22 responses to enteric bacterial pathogens. *Trends Immunol* 2012. **33**: 112-118.

43 **Nunes, T. and de Souza, H. S.,** Inflammasome in intestinal inflammation and cancer. *Mediators Inflamm* 2013. **2013**: 654963.

44 **Shea-Donohue, T., Thomas, K., Cody, M. J., Aiping, Z., Detolla, L. J., Kopydlowski, K. M., Fukata, M., Lira, S. A.,** Mice deficient in the CXCR2 ligand, CXCL1 (KC/GRO-alpha), exhibit increased susceptibility to dextran sodium sulfate (DSS)-induced colitis. *Innate Immun* 2008. **14**: 117-124.

45 **Modan, B., Barell, V., Lubin, F., Modan, M., Greenberg, R. A. and Graham, S.,** Low-fiber intake as an etiologic factor in cancer of the colon. *J Natl Cancer Inst* 1975. **55**: 15-18.

46 **Reddy, B. S.,** Dietary factors and cancer of the large bowel. *Semin Oncol* 1976. **3**: 351-359.

47 **Verspreet, J., Damen, B., Broekaert, W. F., Verbeke, K., Delcour, J. A. and Courtin, C. M.,** A Critical Look at Prebiotics Within the Dietary Fiber Concept. *Annu Rev Food Sci Technol* 2016. **7**: 167-190.

48 **Scheppach, W. and Weiler, F.,** The butyrate story: old wine in new bottles? *Curr Opin Clin Nutr Metab Care* 2004. **7**: 563-567.

49 **Wang, T., Cai, G., Qiu, Y., Fei, N., Zhang, M., Pang, X., Jia, W., Cai, S.,** Structural segregation of gut microbiota between colorectal cancer patients and healthy volunteers. *ISME J* 2012. **6**: 320-329.


This article is protected by copyright. All rights reserved.

Author Manuscript

50 **Kostic, A. D., Chun, E., Robertson, L., Glickman, J. N., Gallini, C. A., Michaud, M., Clancy, T. E., Chung, D. C.,** Fusobacterium nucleatum potentiates intestinal tumorigenesis and modulates the tumor-immune microenvironment. *Cell Host Microbe* 2013. **14**: 207-215.

51 **Sobhani, I., Tap, J., Roudot-Thoraval, F., Roperch, J. P., Letulle, S., Langella, P., Corthier, G., Tran Van Nhieu, J.,** Microbial dysbiosis in colorectal cancer (CRC) patients. *PLoS One* 2011. **6**: e16393.

52 **Trompette, A., Gollwitzer, E. S., Yadava, K., Sichelstiel, A. K., Sprenger, N., Ngom-Bru, C., Blanchard, C., Junt, T.,** Gut microbiota metabolism of dietary fiber influences allergic airway disease and hematopoiesis. *Nat Med* 2014. **20**: 159-166.

53 **Kang, S. G., Wang, C., Matsumoto, S. and Kim, C. H.,** High and low vitamin A therapies induce distinct FoxP3+ T-cell subsets and effectively control intestinal inflammation. *Gastroenterology* 2009. **137**: 1391-1402 e1391-1396.

54 **Barman, M., Unold, D., Shifley, K., Amir, E., Hung, K., Bos, N. and Salzman, N.,** Enteric salmonellosis disrupts the microbial ecology of the murine gastrointestinal tract. *Infect Immun* 2008. **76**: 907-915.

This article is protected by copyright. All rights reserved.

Author Manuscript

**Figure legends**

**FIGURE 1. Acute DSS-induced inflammatory responses in WT and SCFA receptor-deficient mice.** (A) Body weight change (%) and stool score during DSS-induced acute inflammation. (B) Colon length of WT, *Gpr41*$^{-/-}$ and *Gpr43*$^{-/-}$ mice after 3.5% DSS treatment. (C) Frequency of IFN-$\gamma^+$, IL-17A$^+$, and FoxP3$^+$ cells among intestinal lamina propria (LP) CD4$^+$ T cells of WT, *Gpr41*$^{-/-}$ and *Gpr43*$^{-/-}$ mice.. (D) Frequency of Gr-1$^+$CD11b$^+$ cells in colonic LP cells of WT, *Gpr41*$^{-/-}$ and *Gpr43*$^{-/-}$ mice.. (E) Expression of inflammatory cytokine and chemokine genes in colonic tissues of WT, *Gpr41*$^{-/-}$ and *Gpr43*$^{-/-}$ mice. mRNA expression was measured by qRT-PCR and normalized to β-actin (*Actb*). Mice received 3.5% DSS in drinking water for 5 days before they were fed regular water prior to sacrifice at day 9. Representative and pooled data obtained (mean ± SEM, n=8-10) from 2 independent experiments are shown. For panel A, once significant group effects are established, pairwise differences between WT and *Gpr41*$^{-/-}$ or *Gpr43*$^{-/-}$ on days 8 and 9 were separately examined. Group effects were significant for weight change (P=0.0009) and for stool score (P=0.02) with repeated measures ANOVA. *Significant differences from WT with two-sample t-tests with Bonferroni's adjustments for four comparisons (significance at 0.0125 for each). For panel B-E, one-way ANOVA followed by Tukey's multiple comparisons test was used to determine significance between all pairs of groups. *Significant differences between indicated pairs (P<0.05).

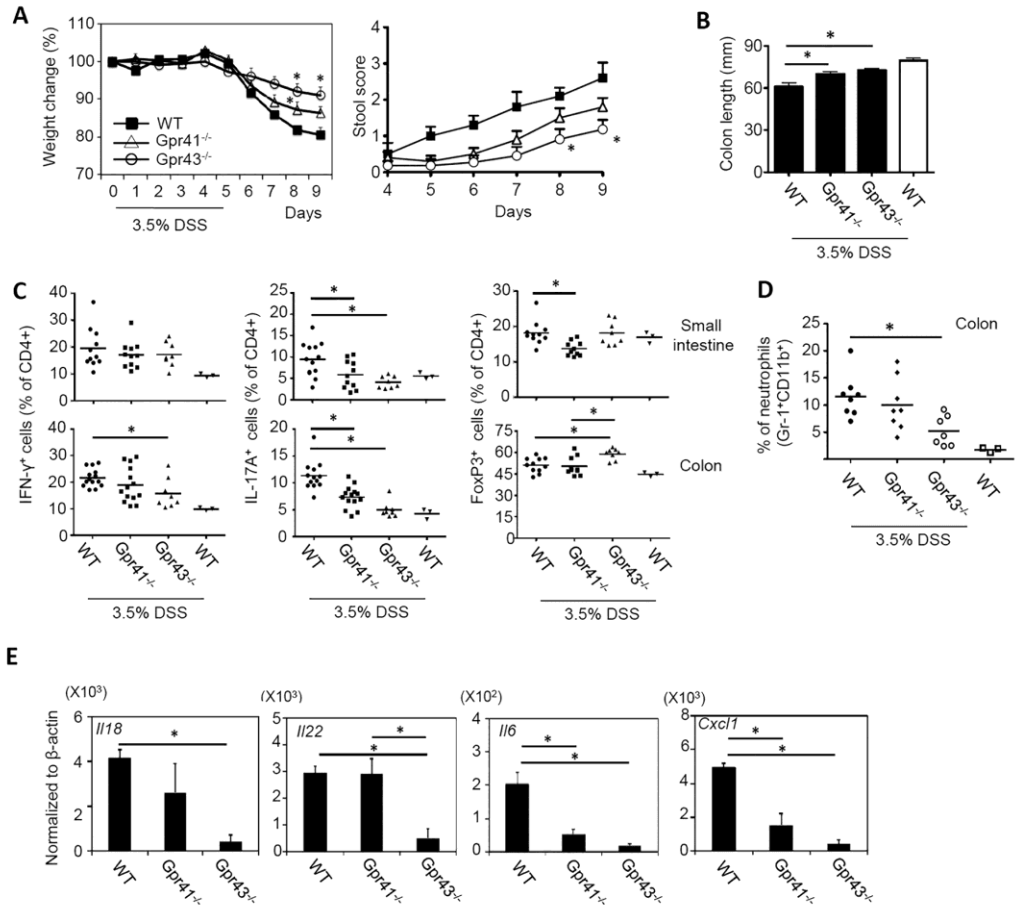


This article is protected by copyright. All rights reserved.

Author Manuscript

**FIGURE 2. Chronic DSS-induced inflammatory responses in WT and SCFA receptor-deficient mice.** (A) Body weight change (%) and stool score during DSS-induced chronic inflammation. (B) Colon length of WT, *Gpr41*$^{-/-}$ and *Gpr43*$^{-/-}$ mice after 3 cycles of 1.5% DSS treatment. (C) Frequency of Gr-1$^{+}$CD11b$^{+}$ cells in the colonic LP cells of WT, *Gpr41*$^{-/-}$ and *Gpr43*$^{-/-}$ mice. (D) Frequency of IFN-$\gamma^{+}$, IL-17A$^{+}$, and FoxP3$^{+}$ cells among LP CD4$^{+}$ T cells of WT, *Gpr41*$^{-/-}$ and *Gpr43*$^{-/-}$ mice. (E) Expression of inflammatory cytokine and chemokine genes in colon tissues isolated from WT, *Gpr41*$^{-/-}$ and *Gpr43*$^{-/-}$ mice. mRNA expression was measured. Mice received 3 cycles of 1.5% DSS for 7 days followed by regular water for 7 days. Representative and pooled data (mean ± SEM, n=8-10) from 2 independent experiments are shown. For panel A, once significant group effects for early and late phases are established, differences between WT and *Gpr41*$^{-/-}$ or *Gpr43*$^{-/-}$ on specific days were separately examined by phases. Significant group effects were seen in early phase (P= 0.034 for weight change and P=0.026 for stools score) and in late phase (P<0.001 for weight loss, and P=0.010 for stool score) with repeated measures ANOVA. Differences from WT were further examined with multiple t-tests on day 11 and 14 of early and day 38 and 40 of late phase for weight change and day 10 and 15 for early and 35 and 40 for late phase for stool score. *Significant difference from WT with Bonferroni's adjustments for four comparisons on each day within each phase (significance at 0.0125 for each). For panel B-E, one-way ANOVA followed by Tukey's multiple comparisons test was used to determine significance between all pairs of groups. *Significant differences between indicated pairs.

This article is protected by copyright. All rights reserved.

Author Manuscript

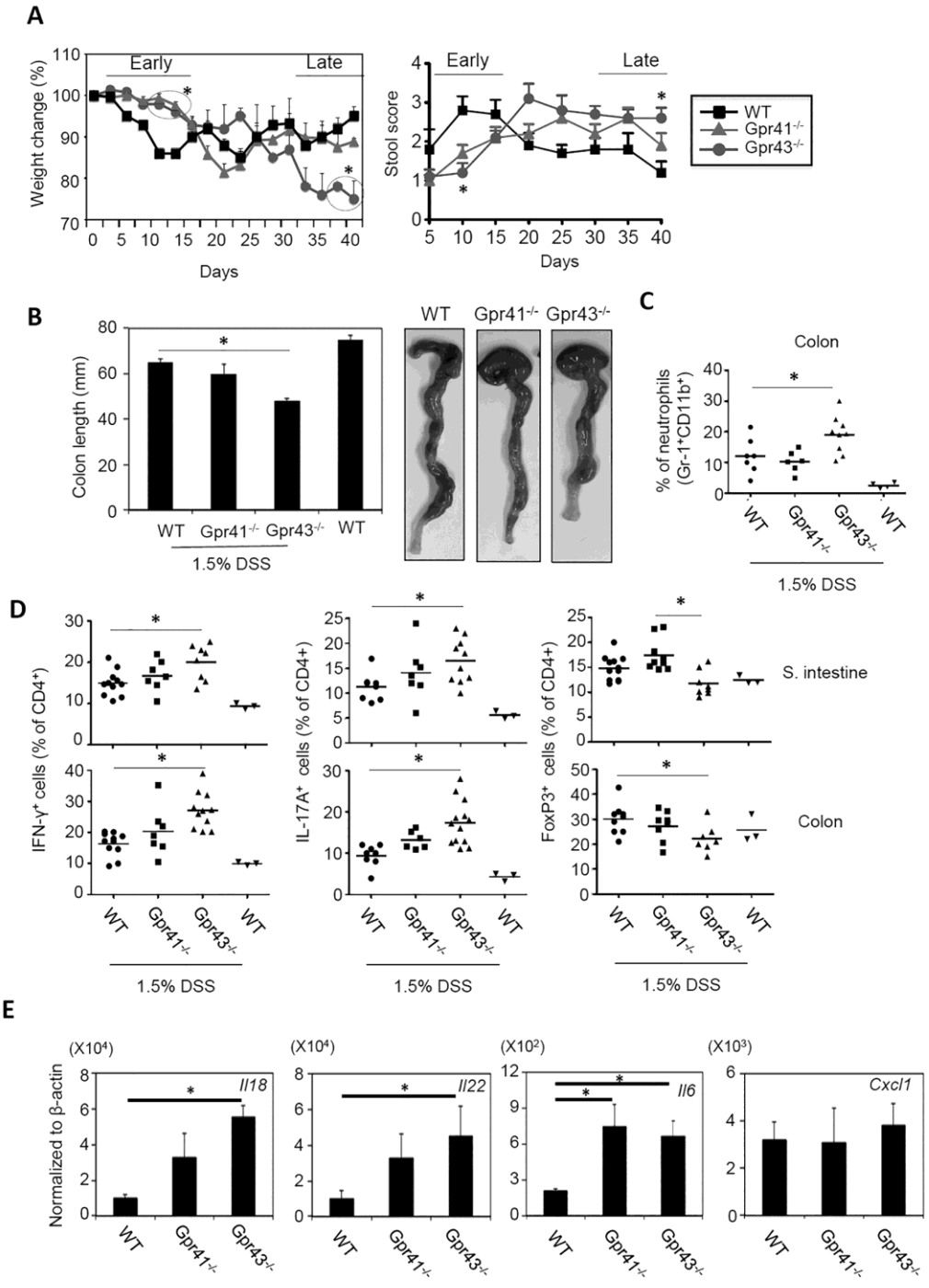


This article is protected by copyright. All rights reserved.

Author Manuscript

**FIGURE 3. AOM/DSS-induced colon cancer development in WT versus GPR43-deficient mice.** (A) Changes in body weight (%), survival rate (%), and stool scores of WT and *Gpr43*$^{-/-}$ mice during AOM/DSS treatment. (B) Tumor burden (adenoma number and size) in the colon of WT and *Gpr43*$^{-/-}$ mice. (C) Histological assessment of colon tissues of WT and *Gpr43*$^{-/-}$ mice. Paraffin-embedded tissue sections (6 μm) were stained with hematoxylin and eosin. Medullary inflammatory cells (I) and necrotic abscesses (N) are marked in the picture. (D) Enlargement of spleen and MLN following AOM/DSS treatment. The broken line indicates average weight of the spleen of untreated age-matching control WT mice. Mice were treated with AOM (10 mg/Kg of body weight, i.p.) and 3 cycles of 1% DSS in drinking water and sacrificed at day 70 post AOM injection. Representative and pooled data (mean ± SEM, n=8-12) from 3 independent experiments are shown. For panel A, significant differences between *Gpr43*$^{-/-}$ and WT were separately examined for early and late phases, followed by pairwise comparisons on specific days with Bonferroni adjustments for multiple comparisons. Differences from WT were further examined using multiple t-tests with Bonferroni's adjustments for 8 comparisons on day 42, 46, 49, and 53 for weight change (significance at $P<0.0063$) and for 4 comparisons on day 3 and 9 in early phase and for 8 comparisons day 43, 48, 53, and 59 in late phase for stool score (significance for each at $P<0.0125$ and $P<0.0063$). *Significant differences from WT obtained with t-tests. For panel B, D, Mann-Whitney U test was performed with * indicating for significant differences ($P < 0.05$).

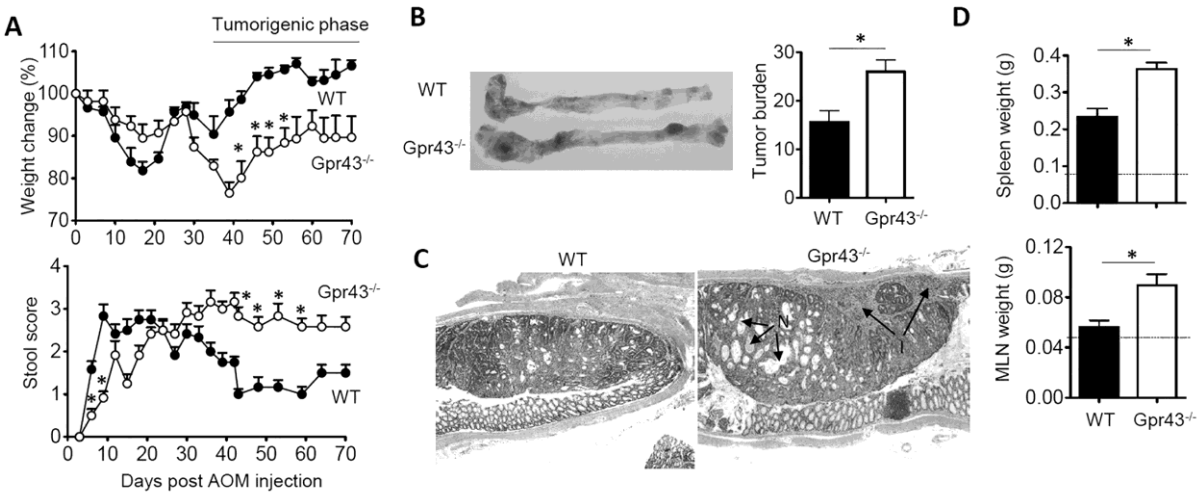


This article is protected by copyright. All rights reserved.

Author Manuscript

**FIGURE 4. AOM/DSS-induced colon cancer development and T cell responses in co-housed GPR43-deficient mice.** (A) Gross colon images of co-housed WT and *Gpr43*$^{-/-}$ mice. (B) Tumor formation (polyp number) in the colon and colon length (mm) of co-housed WT and *Gpr43*$^{-/-}$ mice. (C) Effector T cells, Tregs and neutrophils in the colon of co-housed mice. (D) Spleen weight and T helper cell subset frequencies in the spleen of co-housed mice. (E) MLN weight and effector T cells and Tregs in the MLN of co-housed mice. In panel D and E, the broken lines indicate average weight of the indicated organs of untreated age-matching WT mice. To equalize microbiota between WT and *Gpr43*$^{-/-}$ mice, female mice were co-housed at least one week prior to and until termination of the experiments. Alternatively, male mice were housed on mixed bedding (20% of used bedding equally from WT and *Gpr43*$^{-/-}$ mice and 80% new bedding; changed twice a week). The data from these two experiments were similar and all data were combined. Mice were treated with AOM (10 mg/Kg of body weight, i.p.) and 3 cycles of 1% DSS in drinking water and sacrificed at day 62-63 post AOM injection. Representative and pooled data (mean ± SEM, n=8-12) from 3 independent experiments are shown. *Significant differences ($p < 0.05$, Mann Whitney U test) from AOM/DSS-treated WT mice.

This article is protected by copyright. All rights reserved.

Author Manuscript

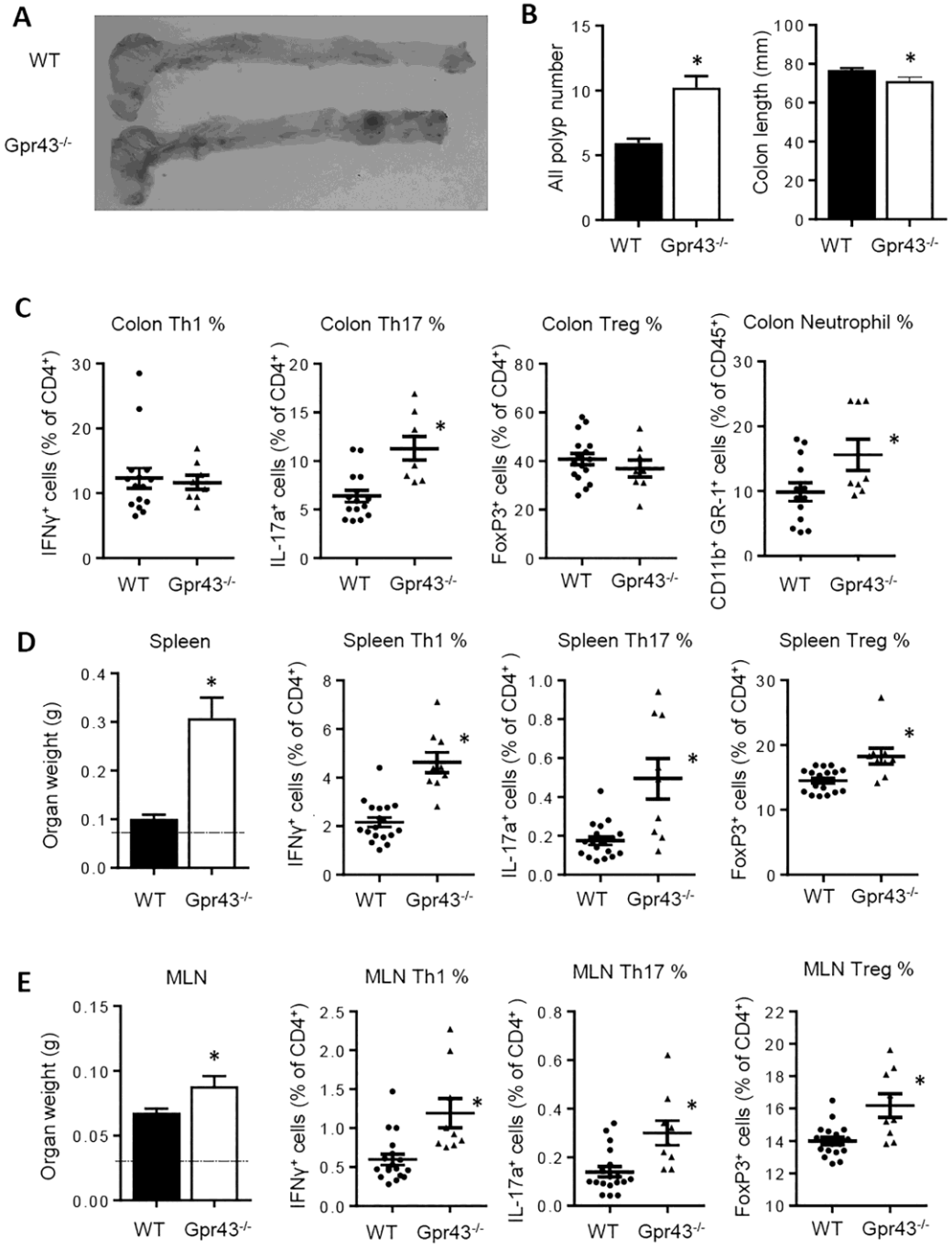


This article is protected by copyright. All rights reserved.

Author Manuscript

**FIGURE 5. Intestinal tumor formation in WT versus *Gpr43*$^{-/-}$ *Apc*$^{Min/+}$ mice.** (A and B) Images and histological assessment of intestine tissues. Tumor formation in the small intestine and colon *Apc*$^{Min/+}$ and *Apc*$^{Min/+}$*Gpr43*$^{-/-}$ mice. (C) Histological assessment of intestine tissues. (D) Enlargement of spleen and MLN in *Apc*$^{Min/+}$ and *Apc*$^{Min/+}$*Gpr43*$^{-/-}$ mice. *Apc*$^{Min/+}$ and *Apc*$^{Min/+}$*Gpr43*$^{-/-}$ mice were sacrificed at 4 months of age. In panel D, the broken lines indicate average weight of the indicated organs of untreated age-matching WT mice. Representative and pooled data (mean ± SEM; n=6) from 2 experiments are shown. *Significant differences from *Apc*$^{Min/+}$ mice ($p < 0.05$, Mann-Whitney U-test).

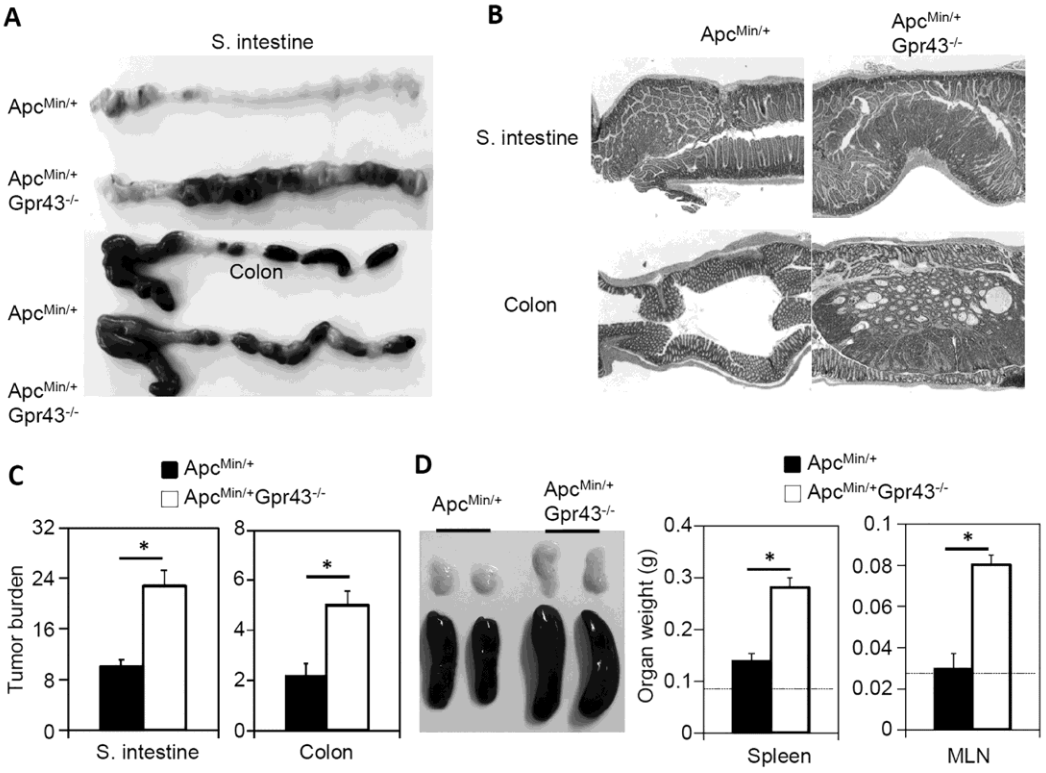


This article is protected by copyright. All rights reserved.

Author Manuscript

**FIGURE 6. Comparison of non-hematopoietic and hematopoietic GPR43 in suppressing colon cancer.** (A) Weight change (%) of mice during AOM/DSS treatment. (B) Tumor formation (number and size) in the colon. (C) Enlargement of spleen and MLN. BM from WT or *Gpr43*$^{-/-}$ mice (10 million cells) were transferred into lethally irradiated WT or *Gpr43*$^{-/-}$ mice, and the chimera mice were treated with AOM/DSS for induction of colon cancer. Chimeras were treated with AOM (10 mg/Kg of body weight, i.p.) and 3 cycles of 1% DSS in drinking water and sacrificed at day 70 post-AOM injection. Representative and pooled data (mean ± SEM, n=7-9) from 2 independent experiments are shown. For panel A, group effect was examined for late phase (days 35-70), and upon establishing significant group effect, pairwise comparisons on specific days (days 55, 60, 65, and 70) were done with Bonferroni adjustments for multiple comparisons. Significant group effect was seen in weight change ($P<0.0001$) using repeated measures ANOVA during late phase. *Significant differences from WT → WT group on days 55-70, obtained with multiple t-tests with Bonferroni's adjustments for 8 multiple pairwise comparisons (significance at $P<0.0063$). For panel B-C, one-way ANOVA followed by Tukey's multiple comparisons test was used to make all pairwise comparisons. *Significant differences between indicated pairs.

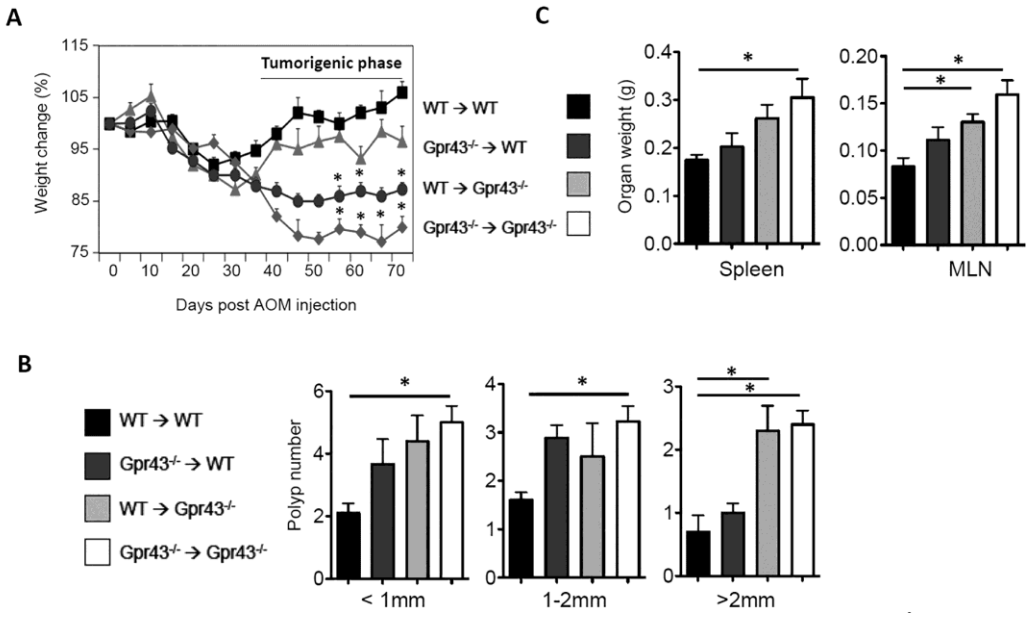


This article is protected by copyright. All rights reserved.

Author Manuscript

**FIGURE 7. Effect of DF on AOM/DSS-induced colon cancer development in WT and *Gpr43*$^{-/-}$ mice.** (A) Colon tissues of WT or *Gpr43*$^{-/-}$ mice fed different levels of DF (LFD, MFD, and HFD) and treated with AOM/DSS. (B) Weight change (%) of WT and *Gpr43*$^{-/-}$ mice during AOM/DSS treatment. (C) Tumor formation in the colon of WT and *Gpr43*$^{-/-}$ mice. Mice were treated by AOM (10 mg/Kg of body weight, i.p.) and 3 cycles of 1% DSS in drinking water and sacrificed at day 70 post AOM injection. Representative and pooled data (mean ± SEM, n=8-10) from 2 independent experiments are shown. For panel B, within each of WT and *Gpr43*$^{-/-}$ type, diet effect was examined for late phase (days 35-70), and when significant effect was established, pairwise comparisons on specific days (65 and 70) were done with Bonferroni adjustments for multiple comparisons. Significant diet effects for late phase ($P<0.0001$) was seen using repeated measures ANOVA in WT mice. *Significant differences from LFD mice on day 65 and 70 with t-tests (significance at $P<0.0125$). For panel C, one-way ANOVA followed by Tukey's multiple comparison test was used to make all pairwise comparisons. *Significant differences between indicated pairs.

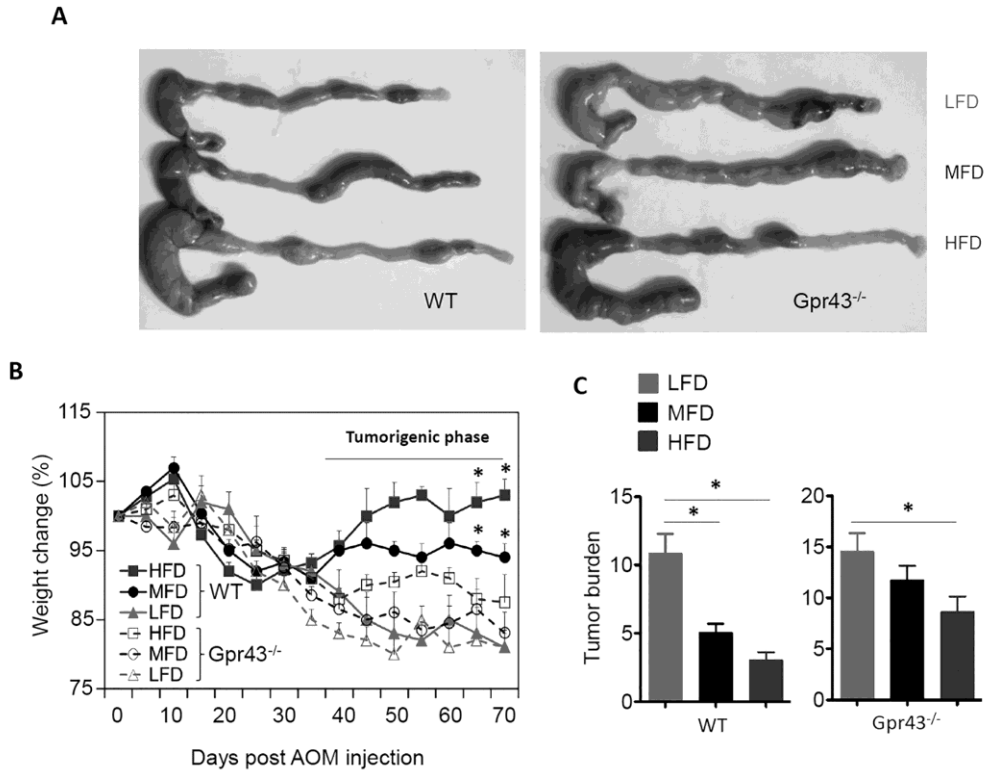


This article is protected by copyright. All rights reserved.

Author Manuscript

**FIGURE 8. Effect of propionate on AOM/DSS-induced colon cancer development in WT and *Gpr43*$^{-/-}$ mice.** (A) Tumor formation in the colon of WT mice fed LFD alone or LFD and C3 (80 mM). (B) Enlargement of spleen following AOM/DSS treatment. (C) Tumor formation in the colon of mice fed indicated diet and drinking water. (D) Histological assessment of colon tissues. Paraffin-embedded tissue sections (6 μm) were stained with hematoxylin and eosin. (E) Spleen enlargement. Mice were fed indicated diet and drinking water and treated with AOM (10 mg/Kg of body weight, i.p.) and 3 cycles of 1% DSS in drinking water and sacrificed at day 70 post AOM injection. Representative and pooled data (mean ± SEM, n=8-12) from 3 independent experiments are shown. For panel A and B, Mann Whitney U test was used for significant differences between two groups*. For panel C and E, in both WT mice and *Gpr43*$^{-/-}$ mice, no interaction of C3 by MFD was found with two-way ANOVA. For both panel C and E, we found significant overall C3 effect (P<.0001 for panel C, P=0.0212 for panel E) and MFD effect (P<0.0001 for panel C, and P=0.0108 for panel E).

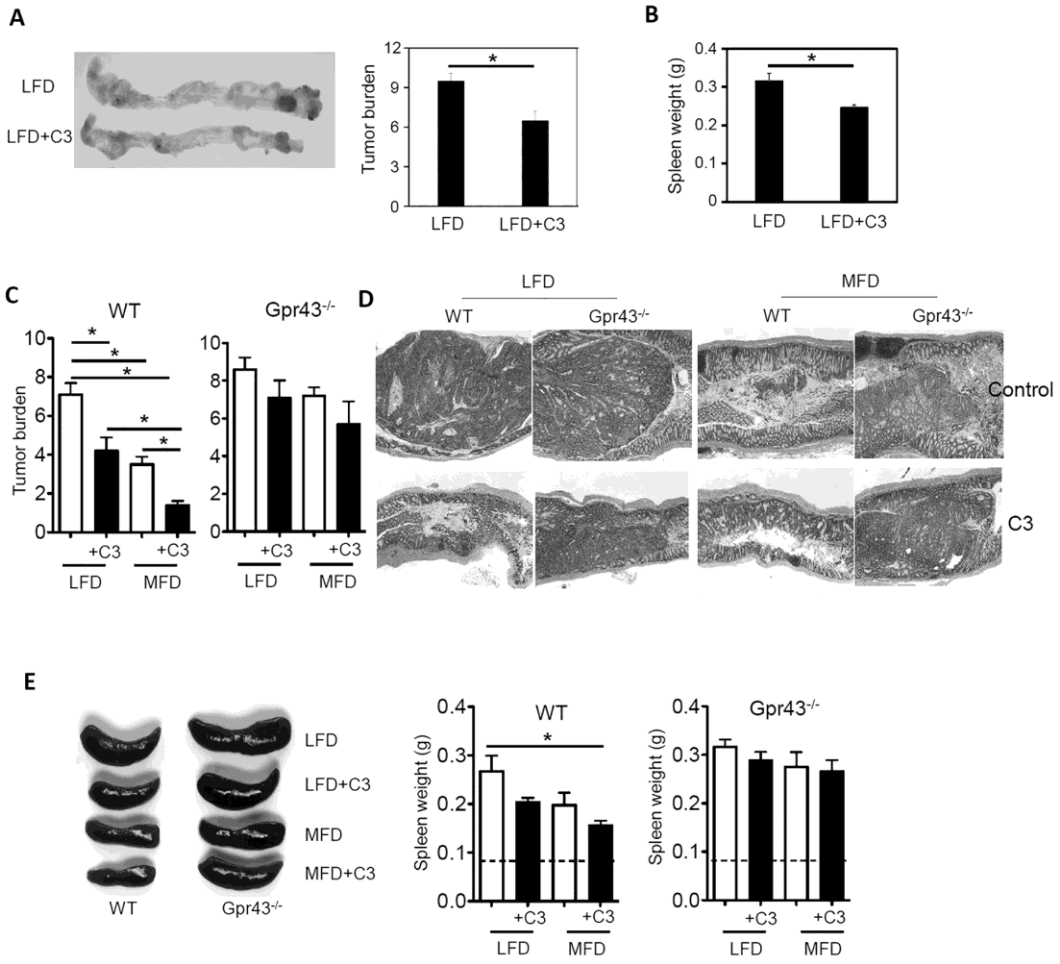


This article is protected by copyright. All rights reserved.

Author Manuscript

**FIGURE 9. Effects of propionate and GPR43 on gut barrier function and tissue bacterial load during inflammation and colon cancer development in WT versus *Gpr43*$^{-/-}$ mice**. In panel A-C, WT and *Gpr43*$^{-/-}$ mice were fed regular rodent chow and C3 (80 mM) in drinking water and treated with 3 cycles of 1.5% DSS and regular water. (A) Expression of tight junction protein genes (*ocln* and *tjp1*) at mRNA level in colon tissues of WT and *Gpr43*$^{-/-}$ mice after DSS treatment. qRT-PCR was performed. (B) Gut permeability in WT and *Gpr43*$^{-/-}$ mice after DSS treatment. Shown is FITC-dextran concentration in blood. (C) Tissue-associated bacteria in the colon following DSS treatment. Confocal microscopy and q-PCR was performed. For q-PCR, DNA isolated from colon tissues was PCR-amplified with primers for total eubacteria and the mouse β-actin gene. Relative levels of eubacterial levels normalized by β-actin gene signals and then by control WT levels are shown. (D) Tissue bacteria load in co-housed mice following AOM/DSS-induced colon cancer. Mice were treated with AOM and 3 cycles of 1% DSS in drinking water and sacrificed at day 16-17 or 62-63 post AOM injection. (E) Tumor formation in the colon from WT and *Gpr43*$^{-/-}$ mice with or without antibiotics (Abx) treatment. Representative and pooled data (mean ± SEM, n=7-9 mice) from 2 experiments are shown. For all panels, two-way ANOVA with an interaction for the two factors was used, and for each panel A, D, and E, a significant interaction term (each P<0.001) was found. Follow-up multiple 2-sample t-tests were done for pair-wise comparisons with Bonferroni adjustment for six pairwise comparisons for each panel. *Significant t-tests at p<0.008. For panel B and C, interaction of C3 by Gpr43 was not significant for both gut permeability and for tissue bacteria. Two-way ANOVA with main factors only found significant Gpr43 (P<0.0001) and C3 (P=0.042) effect for gut permeability (B) and significant Gpr43 (P<0.0001) and C3 (P=0.0022) effects for tissue bacteria (C).

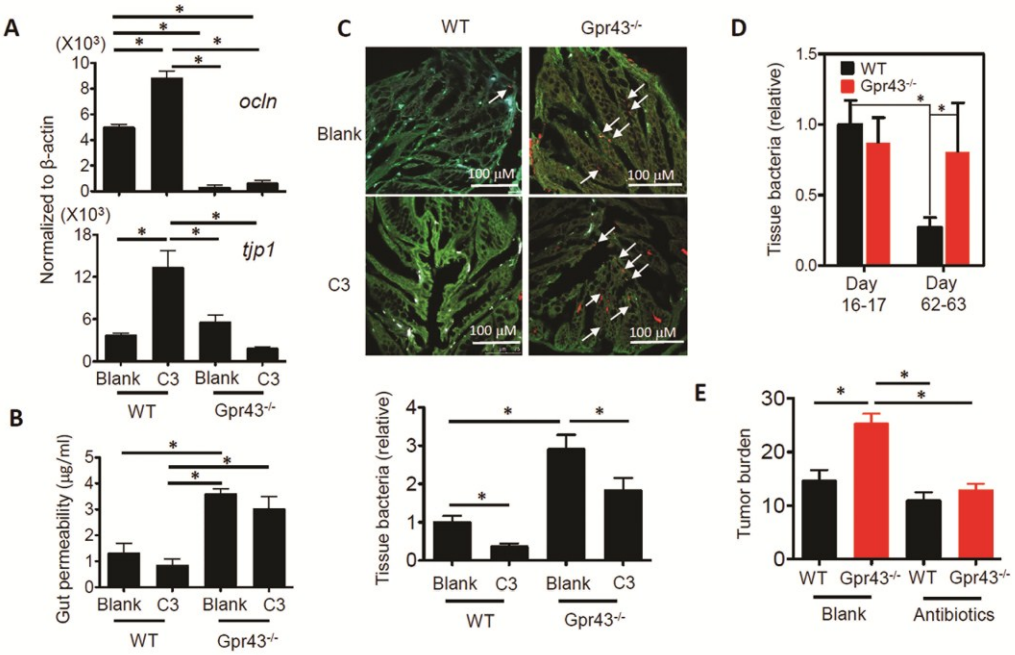


This article is protected by copyright. All rights reserved.